Atomic flux measurement by diode-laser-based atomic absorption spectroscopy

Weizhi Wang,[a] R. H. Hammond, M. M. Fejer, and M. R. Beasley
Edward L. Ginzton Laboratory, Stanford University, Stanford, California 94305

(Received 5 May 1999; accepted 6 June 1999)

Diode-laser-based atomic absorption (AA) sensors have been developed for direct measurement of atomic flux, based on both atomic density and velocity information, which is important for *in situ* monitoring and control of physical vapor deposition processes. Laser beam schemes based on the Doppler shift measurement have been designed for measuring the velocity component normal to the surface of a substrate. Experimental results on electron-beam evaporated barium and yttrium, which are components in YBCO superconductor, demonstrate measurements of true flux instead of simple density in the deposition processes. The flux measurement was confirmed at different pressures showing true flux measurement independent of background pressure. A model-independent flux measurement was achieved by using a cross-beam scheme. In addition, the AA sensor was also used for diagnosing and helping better understand the deposition physics such as sticking coefficient, velocity of the evaporated atoms, and the oxidation of the elements on the substrate. Discussion on practical issues of the AA sensor application is also presented. © *1999 American Vacuum Society.* [S0734-2101(99)08405-5]

I. INTRODUCTION

In situ monitoring and control of the physical vapor deposition (PVD) process are required for a variety of applications, including high-performance alloys, high temperature superconductors, metallization of semiconductor devices, photovoltaic materials, and thermal barrier coatings. Most industrial thin film syntheses use measurement of the deposition rate, which is proportional to the mass flux or atomic number flux of the species, for characterizing and controlling the deposition process. Furthermore, in multicomponent films composition control is also important, so noninvasive and element-specific flux measurement is required for advanced thin film synthesis.

While there are several types of monitors being conventionally employed for PVD processes, such as quartz crystal monitors (QCM),[1] quadrupole mass spectrometers (QMS),[2] ion gauges,[3] and electron impact emission spectrometers (EIES),[4] none of them satisfy all the above-mentioned requirements, and only the QCM measures the flux. Lamp-based atomic absorption (AA) sensors have been successfully developed[5] and commercialized,[6] but measure only the atomic density. The virtue of the lamp-based systems is that the light sources are available for almost all the technologically interesting solid state elements. However, lack of velocity information makes the measurement deviate from the true flux, which can be serious in some applications. In addition, the incoherent light source limits the system performance.

In contrast, AA spectroscopy with highly coherent lasers,[7] in particular, commercially available external cavity diode lasers (ECDL), has many advantages: (1) they are simultaneously both element specific and noninvasive; (2) they can measure the atomic flux, which contains information on both density and velocity, rather than simply the density, for precise process control and study of the deposition process; (3) the AA measurement provides a line-integration signal containing the information about the spatial distribution of the flux over the entire substrate region rather than at a point; (4) the narrow spectral linewidth and tunability of the diode laser allow a range of advanced spectroscopic techniques to be employed for increasing sensitivity, correcting system drift, and measuring optically thick vapors; (5) the high optical power allows the use of solid state detectors, and in principle allows multiplexing the laser beam probe to multiple locations in the deposition system for tomographic imaging; (6) the integration and interface of multiple element-specific systems with the vacuum chamber is easy. The only extra requirement compared to conventional monitors is the optical access windows in the deposition chamber, if feedthrough optical fibers are not used.

In this article, we report the development of diode-laser-based AA monitors for *in situ* rate control. Experimental results on electron-beam (e-beam) evaporated barium and yttrium, which are components of YBCO superconducting thin film, are presented as examples showing the potential for study of deposition physics and *in situ* deposition rate control.

II. DIRECT ATOMIC FLUX MEASUREMENT

A. Atomic flux in the deposition process

The deposition rate R (Å/s) is defined as

$$R = km\Gamma_{\text{in}}/\rho, \tag{1}$$

where k is the sticking coefficient, m is the atomic mass, ρ is the density of the deposited film, and Γ_{in} is the atomic flux defined as:

$$\Gamma_{\text{in}} = n\langle v_z \rangle, \tag{2}$$

[a]Electronic mail: wwang@loki.stanford.edu

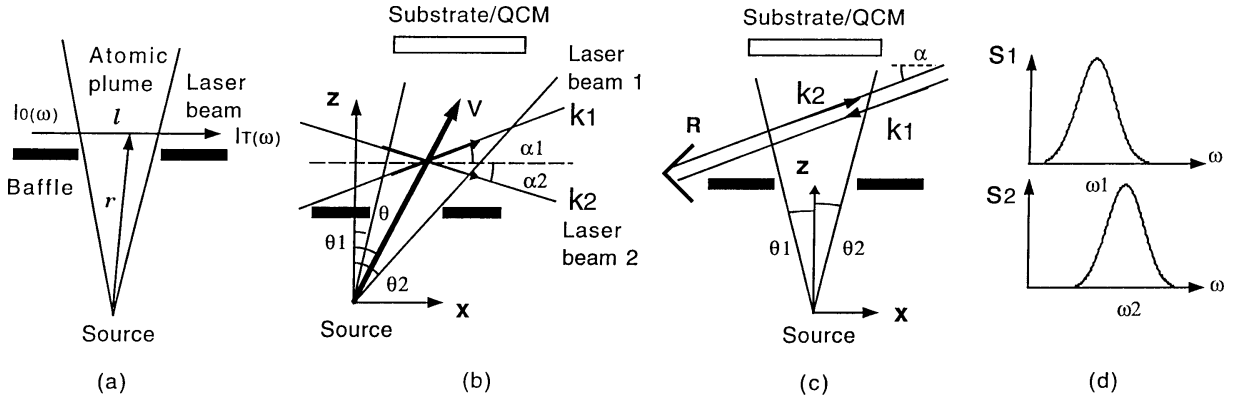

FIG. 1. Schematic showing the principle of density and normal velocity component measurements. (a) Density measurement by using Beer's law, ω is the optical frequency, $I_0(\omega)$ is the incident laser intensity which usually remains constant when the frequency is scanned, $I_T(\omega)$ is the transmitted laser intensity, r is the position vector representing a position along the absorption path, and l is the absorption path length. The atomic plume is apertured by a baffle. (b) Cross-beam scheme, k_1 and k_2 are wave vectors of the two laser beams, α_1 and α_2 are angles between two laser beams and the line parallel to the substrate surface, θ_1 and θ_2 are angles between the z axis and the respective outer boundaries of the atomic plume confined by the baffle, θ is an arbitrary angle between the z axis and the discussed atomic beam; and v is the velocity of atoms. A QCM is placed in the position of the substrate to serve as a reference in the experiments. (c) Counter-propagating-beam scheme, R is a retroreflector; (d) Absorption profiles, S_1 and S_2, seen by the respective laser beams, and ω_1 and ω_2 represent positions of the first moments of the two absorption profiles in frequency, respectively.

where n is the mean atomic number density, $\langle v_z \rangle$ is the mean velocity component of the incoming atoms normal to the substrate. It can be seen that a precise measurement of the deposition rate requires simultaneously precise measurements of the atomic number density, the mean normal velocity component, and the sticking coefficient for a given atomic species.

The sticking coefficient can be defined as

$$k = 1 - \frac{\Gamma_{\text{out}}}{\Gamma_{\text{in}}}, \tag{3}$$

where Γ_{out} is the atomic flux outgoing from the substrate. The outgoing atoms from the substrate are attributed to a reevaporation process, which contains all contributions including elastic and inelastic collisions of the evaporated atoms with the substrate, evaporation of the deposited atoms from the substrate due to heating, and so on. Such a process is a complicated function of the substrate surface conditions, energy of the incident atoms, and also the background gas compositions.

For atoms with nearly unity sticking coefficient, which is usually satisfied at low substrate temperatures or in reactive deposition processes, it is often adequate to assume $k=1$, but simultaneous measurements of both density and velocity are still necessary to determine the flux.

B. Flux measurement based on AA spectroscopy

Measurements of both atomic density and the velocity of a particular element are performed by measuring the basic AA spectroscopic feature, i.e., the absorption profile, which is the absorption coefficient versus optical frequency. Based on Beer's law [referring to Fig. 1(a)], we have

$$I_T(\omega) = I_0(\omega) \exp\left[- \int_l s(\omega, r) dl \right], \tag{4}$$

where ω is the optical frequency, $I_0(\omega)$ is the incident laser intensity, $I_T(\omega)$ is the transmitted laser intensity, $s(\omega, r)$ is the absorption coefficient. The line average absorption coefficient at frequency ω, defined as

$$S_i(\omega) \equiv \frac{1}{l} \int_l s_i(\omega, r) dl = \frac{1}{l} \ln\left[\frac{I_0(\omega)}{I_T(\omega)} \right], \tag{5}$$

can be obtained by measuring $I_T(\omega)$, $I_0(\omega)$ and l; $i=1,2$ correspond to the two laser beams respectively, and l is the absorption path length.

The atomic density is proportional to the area under the absorption profile,[8] i.e.,

$$\int s(\omega, r) d\omega = \frac{\lambda^2 g A}{4} n(r), \tag{6}$$

where λ is the wavelength, g is the ratio of the statistical weights of the two levels involved in the absorption, A is the Einstein spontaneous emission coefficient of the excited state, and $n(r)$ is the difference of the local atomic population densities between the two energy levels. Therefore, according to Eqs. (5) and (6), we have

$$\bar{n} \equiv \frac{1}{l} \int_l n(r) dl = \frac{4}{g A \lambda^2} \int S(\omega) d\omega, \tag{7}$$

which implies that we can obtain the line average density, $\bar{n}$, which is used as the mean atomic density to calculate the flux, by integrating $S(\omega)$ over the entire absorption spectrum with sufficient knowledge of the atomic spectra of the levels involved in the absorption.

Because excited state populations are often strongly dependent on process parameters, usually, ground state transitions have to be used in order to simplify the calibration or interpretation of the measured atomic population difference to the atomic number density in deposition process.

In order to measure directly the normal component of the velocity, a scheme with two optical beams from the same laser (cross-beam scheme), delivered into the atomic plume with angles α_1 and α_2 to the substrate surface, is used as shown in Fig. 1(b). The measurement principle is explained as follows.

Considering a collimated atomic beam with an angle θ to the z axis, the sum of the two absorption profiles, $S_T(\omega)$, seen by the two laser beams contains two sharp peaks in the frequency domain and can be expressed as

$$S_T(\omega)=S_1(\omega-\mathbf{k}_1\cdot\mathbf{v})+S_2(\omega-\mathbf{k}_2\cdot\mathbf{v}), \tag{8}$$

where $\mathbf{k}_1\cdot\mathbf{v}$ is the Doppler shift.

Generally, the frequency separation between the two peaks, which is the relative Doppler shift, in these two absorption profiles is given by

$$\Delta=(\mathbf{k}_1-\mathbf{k}_2)\cdot\mathbf{v}=(k_{1x}-k_{2x})v_x+(k_{1z}-k_{2z})v_z \tag{9}$$

determined by both v_x and v_z, which are the velocity components along and perpendicular to the substrate surface, respectively. When $k_{1x}=k_{2x}$, $k_{1z}=-k_{2z}$, corresponding to $\alpha_1=-\alpha_2$ in Fig. 1(b), the frequency separation

$$\Delta=2k_{1z}v_z, \tag{10}$$

is independent of v_x, and therefore v_z can be obtained by measuring Δ.

A real atomic plume has a finite angular spread in space and the atomic velocity has a distribution instead of a constant value, resulting in a spectral spread in the absorption profile due to the Doppler broadening. As long as we keep $\alpha_1=-\alpha_2$, Eq. (10) holds for atoms with any value of θ. Therefore, we have

$$\langle\Delta\rangle=\langle\omega_1\rangle-\langle\omega_2\rangle=2k_{1z}\langle v_z\rangle, \tag{11}$$

implying that the ensemble average value of v_z, $\langle v_z\rangle$ can be obtained by measuring the separation between the two first moments of the two absorption profiles, where the first moment of the absorption profile is defined as

$$\langle\omega_i\rangle=\frac{\int\omega S_i(\omega)d\omega}{\int S_i(\omega)d\omega}. \tag{12}$$

From Eqs. (11) and (12), the calculation of $\langle v_z\rangle$ from the measured absorption profiles is simple and straightforward, requiring no further information on the lineshape function, which indicates that this scheme provides a model independent flux measurement, as long as the two beams encounter statistically identical samples of the atomic plume. In order to make the two laser beams sample the same group of atoms, close to the substrate in the deposition process, only a small angle α is permitted.

In practice, the two absorption profiles can be detected either with two separate detectors or with one detector by optically combining the two laser beams before sending them to the detector. In the one detector scheme, because of the Doppler broadening, the two absorption profiles may not be well separated but overlapped. Decomposing the contribution of the respective profiles from the overlapped spectrum in the frequency domain usually requires a line shape function for the absorption profile and curve-fitting process, leading to a model-dependent data processing for the flux measurement. Thus, the use of two detectors offers a more robust measurement, at the expense of slightly more complex hardware requirements.

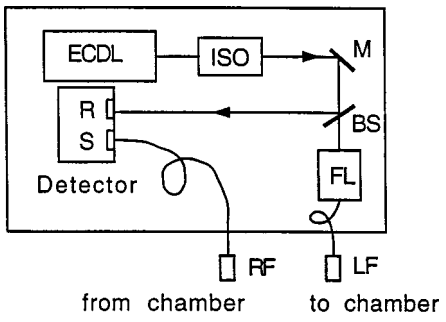

FIG. 2. Configuration of the diode-laser-based AA sensor. ECDL, external cavity diode laser; ISO, optical isolator; M, mirror; BS, beam splitter; FL, fiber launcher; RF, receiving fiber with collimator package; LF, launching fiber with collimator package; R and S in the detector represent reference and signal channels of the autobalanced detector (New Focus 2007), respectively.

Another special laser beam geometry is the counter-propagating-beam scheme, i.e., $\mathbf{k}_1=-\mathbf{k}_2$, consisting two counter-propagating laser beams with a tilting angle α shown in Fig. 1 (c). In this case, we have

$$\langle\Delta\rangle=2k_{1x}\langle v_x\rangle+2k_{1z}\langle v_z\rangle. \tag{13}$$

For a plume symmetric around z axis, which is actually the case for many applications, $\langle v_x\rangle=0$, implying that we can still obtain $\langle v_z\rangle$ by measuring the difference in the moments of the two absorption profiles. In the case that the line shape of each absorption profile is symmetric with respect to its mean, then the distance between the two moments in frequency is simply the distance between two peaks in the spectrum. Although the counter-propagating-beam scheme requires a symmetric plume and a curve-fitting process, it can be incorporated with the one detector scheme conveniently, in which only one laser beam has to be delivered to the atomic plume, a retroreflector can be employed in or outside the deposition chamber so as to form the second laser beam automatically. The advantage of this scheme is that it requires fewer optical and electronic components than in the two-detector scheme, and reduces the number of optical ports required in the vacuum system.

III. EXPERIMENTAL RESULTS AND DISCUSSION

A. Experimental setup

The spectroscopic technique employed in this article was based on wavelength modulation spectroscopy and autobalanced detection, allowing for high sensitivity, wide dynamic range, and low drift using simple electronics and requiring a minimum number of components, [9] as shown in Fig. 2. This detection scheme also provides an output proportional to the power of the signal channel that can be used to normalize changes in the system transmission due to contamination of

chamber windows, variations of coupling efficiencies of optical devices, etc. The combination of autobalanced detection and wavelength modulation reduced baseline artifacts in the spectroscopic technique to a typical level equivalent to an absorption of 10^{-5}. The dominant source of the instrumental uncertainty was the uncorrected étalon fringes caused by reflections from the optical surfaces in the system. The sensor can be easily interfaced with a deposition chamber by using optical fibers.[9]

The output signal from the sensor is proportional to the first derivative of the absorption profile for a given atomic absorption species. In order to obtain the absorption profile, throughout the experiments the center frequency of the laser was scanned at a frequency of 1 Hz over a range of a few GHz centered on the absorption peak, to recover the entire absorption line.

It should be pointed out that the wavelength modulation scheme employed in this article was designed for measurement of weak absorptions, i.e., for applications in which either the deposition rate is low or the atomic transition is weak. Although the dynamic range of absorption measurement is large in the wavelength modulation approach, it is not a necessary choice in the case of large absorption, for which a scheme with direct frequency scan can be good enough to obtain the absorption profile. In addition, the direct frequency scan approach has the advantage that it offers a nonzero baseline which can be used for calibration of the absolute absorption value. Intensity modulation can be applied to incorporate phase sensitive detection to further suppress the noise.

B. Barium

1. Counter-propagating-beam scheme

Atomic flux measurements with AA monitors at 791 nm ground state transition ($^1S_0-^3P_1$) for barium was performed in an e-beam evaporation chamber. As shown in Fig. 1(c), a counter-propagating-beam scheme was used with a retroreflector installed inside the chamber. The tilting angle α was 11°. The e-beam evaporated atomic plume was configured to be symmetric about the z axis with $\theta_2=-\theta_1=5°$ by using baffles. To separate the contributions to the absorption seen by the two laser beams so as to measure the Doppler shift, curve fitting was performed to the first derivative signal, assuming a Gaussian line shape for each absorption component because the linewidth was dominated by the residual Doppler broadening in our experiment. The mean normal velocity component is calculated from the distance between peaks of the two Gaussian profiles. The atomic flux is obtained by the product of measured velocity component and density. The atomic flux was measured simultaneously by the QCM placed above the laser beams for comparison.[10]

To demonstrate the effectiveness of the current flux measurement scheme, which should be independent of the background gas pressure, we changed the background gas pressures during the evaporation by putting argon gas into the deposition chamber. Figure 3 shows the relationship between the QCM rate and the measured flux with the AA sensor.

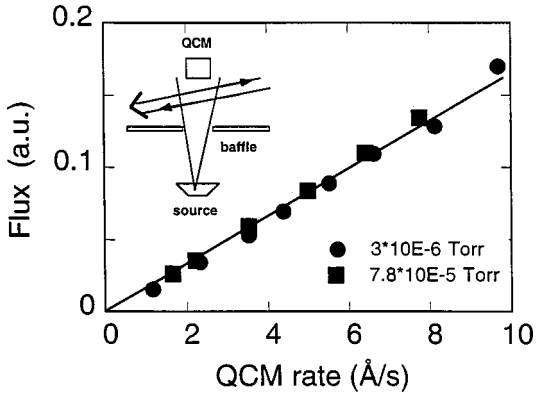

FIG. 3. Measured flux with the AA sensor vs the QCM rate at different background pressures. The background pressure was changed by putting argon gas. The inset shows the configuration.

The measured flux agreed well at different pressures ranging from 3×10^{-6} to 7.8×10^{-5} Torr, which is usually employed in reactive co-evaporation processes, e.g., for the YBCO superconducting thin film. In all of the data shown in this article, the slight deviations of the measured values from the line are due to the noise in the QCM. The effect of pressure will be discussed later.

The AA sensor is also a useful tool to help diagnose the evaporation process and study the deposition physics. Figure 4 shows the typical velocity measured by the Doppler shift as a function of rate measured by the QCM. The velocity of the e-beam evaporated atoms increased about 20% in a relatively small rate range (2–10 Å/s). This increase of the velocity is larger than that caused by the increase of the source temperature required in the case of thermal equilibrium vapor for higher rate. It evidently shows that the e-beam evaporation source is not a thermal equilibrium source. In such an evaporation process, the e-beam evaporated atoms expand quickly in the vacuum, and experience an adiabatic cooling

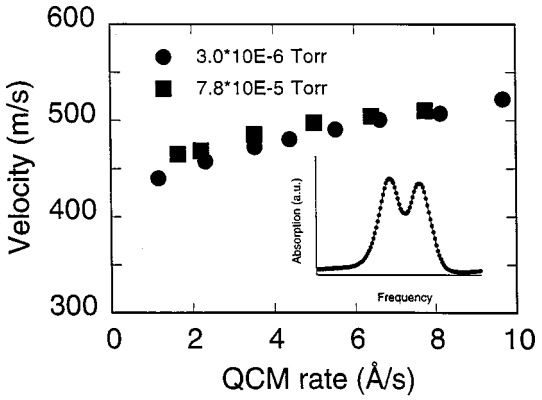

FIG. 4. Measured velocity of barium in the e-beam evaporation vs the QCM rate at different background pressures. Note that the velocity shows a significant dependence on both deposition rate and pressure. The inset is the lineshape seen by the two counter-propagating laser beams received at one detector. The lineshape is obtained by integrating, with respect to the frequency, the derivative output from our AA sensor.

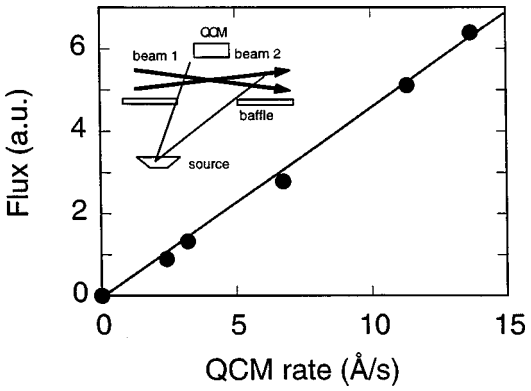

FIG. 5. Measured flux by AA sensor vs the QCM rate. The inset is a schematic showing the geometry of the laser beams, atomic plume and the QCM in the cross-beam scheme.

during the expansion, resulting in a higher flow velocity.[11,12] In order to measure precisely the atomic flux in a large dynamic range, it is necessary to measure the flux instead of a simple density.

2. Cross-beam scheme with one detector

A cross-beam scheme with one detector was constructed by using mirrors inside the chamber to complete the laser beam loop, satisfying $k_{1x}=k_{2x}$ and $k_{1z}=-k_{2z}$ with $\alpha_1=-\alpha_2=11°$. To test the validity of the scheme with a difficult case, the atomic plume was apertured to produce a large tilting angle to the substrate normal with $\theta_1=14°$ and $\theta_2=27°$ [referring to Fig. 1(b)]. Curve-fitting was used by assuming Gaussian shapes with different height and width due to the different Doppler broadening seen by each laser beam. Figures 5 and 6 are measured flux, density, and velocity versus the deposition rates measured by the QCM placed above the cross point of the two laser beams. The deviation of the density from a linear dependence on the rate shows again that a simple density measurement could have a significant deviation from the true flux.

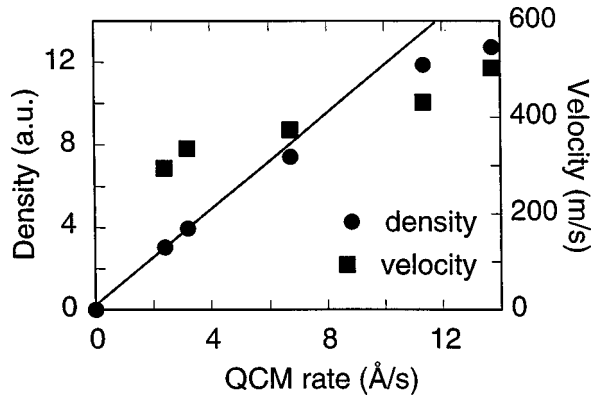

FIG. 6. Measured density and velocity by the AA sensor vs the QCM rate. Note the deviation of the measured density from the line and the significant increase in velocity.

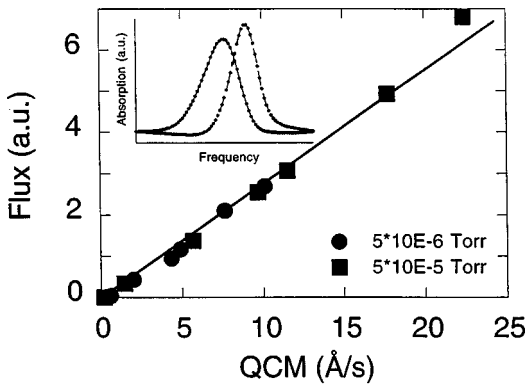

FIG. 7. Measured flux by the AA sensor vs the QCM rate at different background pressures. The background pressure was changed by putting argon gas into the chamber. The deviation of the measured value from the line at higher rate was due to the scattering effect and is discussed later in the text. The inset shows the separate two absorption profiles detected at two detectors. Two absorption profiles were obtained respectively from integrating the derivative outputs in the two detectors of the AA sensor.

3. Cross-beam scheme with two detectors

To demonstrate model-independent flux measurement, a cross-beam scheme with two separate detectors was constructed by using a fiber coupler with 50/50 split ratio to form two separate laser beams. The atomic plume was the same as in the cross-beam scheme with one detector. The two laser beams with $\alpha_1=-\alpha_2=10°$ pass through two pair of windows and are coupled into two separate receiving fibers to send to two detectors. Two separate lock-in amplifiers with the same reference frequency are used. Because the two absorption profiles are separated electronically, the signal processing to calculate the area under the absorption profile and the difference in moments of the two absorption profiles are simple and fast, requiring no detailed knowledge about the spectrum.

Figure 7 shows the comparison between the deposition rates measured by the AA sensor and the QCM placed above the cross point of the laser beams. Pressure independence was also confirmed by putting argon gas in the chamber up to 5×10^{-5} Torr.

Another interesting result of flux measurement is shown in Fig. 8. The two sets of data are results with background gas pressure $<5\times10^{-6}$ Torr, and at oxygen pressure 5×10^{-5} Torr. The different slope indicates that oxidation of Ba forms BaO on the surface of the QCM when the background gas is molecular oxygen, changing the apparent QCM deposition rate calibrated for Ba metal. The ratio of the two slopes of about 1.35 differs from the nominal ratio of BaO to Ba in the calibration of the QCM which is 1.46, implying that a partial oxidation of Ba took place at this oxygen pressure.

4. Sticking coefficient

The sticking coefficient on the substrate of certain species in thin film synthesis may vary under different substrate surface conditions. To demonstrate the possibility of *in situ*

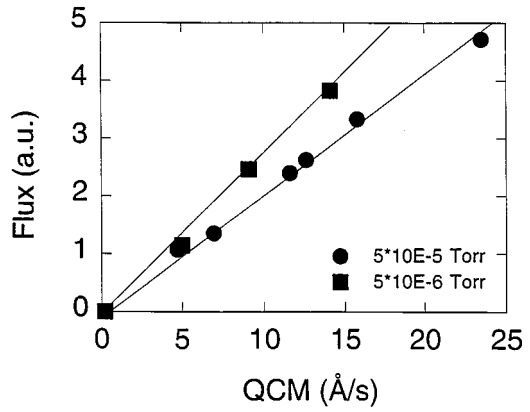

FIG. 8. Measured flux by the AA sensor vs. the QCM rate calibrated for Ba metal. The background pressure at 5×10^{-5} Torr was obtained by putting oxygen gas into the chamber. Different slopes show the effect of the oxidation of Ba on the QCM surface. The ratio of the two slopes is 1.35.

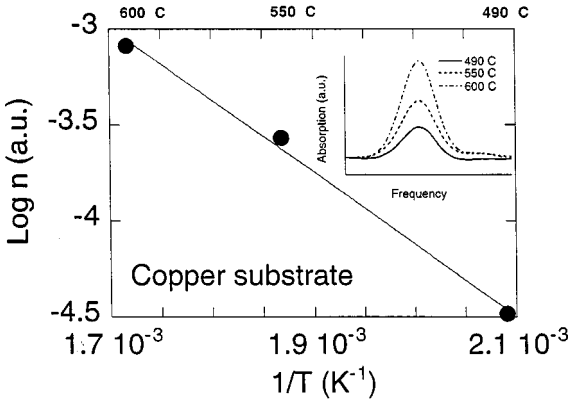

FIG. 10. Measured density vs $1/T$, showing the re-evaporation process of Ba from a copper substrate as a function of temperature. The e-beam source was off during the measurement. The inset shows correspondingly the integrated absorption profiles obtained from the re-evaporated atoms when the substrate temperature was changed.

measurement of the sticking coefficient with the AA sensor, a scheme with a single-pass laser beam was employed for barium deposition on a copper substrate (see the inset of Fig. 9). The tilting angle of the laser beam with respect to the substrate surface was 11°. The copper substrate attached with a heater was installed just above the laser beam. The temperature of the substrate was measured by a thermocouple embedded in the substrate for closed-loop temperature control. Figure 9 shows the measured absorption line shape. In this experiment, the deposition rate was about 10 Å/s. A sharp peak corresponds to the evaporated atomic beam from the source, a broad shoulder seen in the absorption profile indicates that barium atoms were re-evaporated from the substrate. The frequency shift between the centers of the sharp and broad peaks was due to the Doppler shift of the evaporated atomic beam seen by the tilted laser beam. By using curve fitting with two Doppler-shifted Gaussian components assigned to the absorption profiles due to the evaporation and the re-evaporation, the temperature was estimated, from the width of the broad re-evaporation line shape, to be 637 °C by assuming the re-evaporated atoms have an isotropic velocity distribution, agreeing well with the temperature measured by the thermocouple at the substrate which was 600 °C. The sticking coefficient of the barium on the copper surface at 600 °C was found to be 63% according to Eq. (3) where $\langle v_z \rangle$ in Γ_{in} was calculated by the Doppler shift measured through curve fitting, while $\langle v_z \rangle$ in Γ_{out} was calculated by averaging the isotropically distributed velocity determined by the temperature.

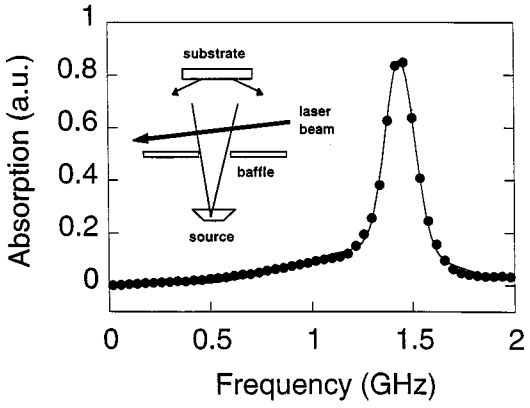

FIG. 9. Integrated line shape from the AA sensor, containing a sharp peak due to the directional evaporated Ba atomic beam from the source and a broad one with shifted center due to the isotropically re-evaporated atoms from the substrate. Dots are experimental data and the solid line is the fitted curve. The inset is the configuration for the sticking coefficient measurement. A copper substrate was attached to a heater.

To confirm the re-evaporation process, the barium source was shut off after substantial barium atoms were accumulated on the substrate at low temperature, thereafter the substrate was heated up. Absorption signals were obtained during the heating. Figure 10 shows that the density of the re-evaporated atoms obtained from the absorption signal increased exponentially with increasing the substrate temperature. However, large density variations at fixed temperature were observed, suggesting the complexity of the re-evaporation process affected by the substrate surface conditions, background gas compositions, and so on.

The present result indicates that the laser-based AA monitor can be used for *in situ* sticking coefficient measurement which is important for a complete measurement of the deposition rate in the thin film synthesis, when the assumption of a unity sticking coefficient is not valid.

C. Yttrium

The counter-propagating-beam scheme was also employed for experiments with e-beam evaporated yttrium. The experimental configuration was the same as used in the counter-propagating-beam scheme for Ba. The situation in yttrium is more complicated than in barium due to the existence of a metastable level which is 530 cm^{-1} above the ground state.[9] At temperatures characteristic of the evaporation, this metastable level was substantially populated. How-

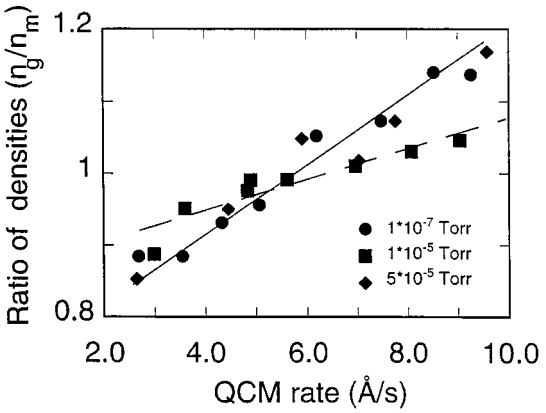

FIG. 11. Relation between the ratio of the populations in the two levels and the QCM rate at different background pressures. Lines are meant to guide the eye. n_g and n_m are the densities at the ground state and the metastable level, respectively.

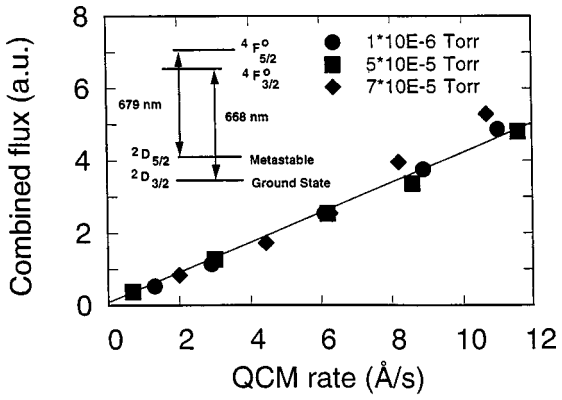

FIG. 12. Combined flux vs the QCM rate at different background pressures. The background pressure was changed by putting argon gas. The deviation of the data from the line is discussed in the text. The configuration was the same as in Fig. 3.

ever, the ratio of the ground state population to the metastable level population was not a constant when the evaporation conditions, e.g., the rate, the e-beam spot size and location, the source surface, or the background gas pressure, changed. To characterize the influence of the metastable level, measurements of these two levels with two separate lasers at 668 and 679 nm were carried out. The sensor scheme for each wavelength is the same as for barium. Laser beams from the two lasers were combined by coupling them into one optical fiber and delivered into the chamber. In the measurement, the two laser beams were chopped alternately in time. Atomic flux corresponding to the ground state and metastable levels was thus measured for a few seconds alternately.

The absorption spectrum of yttrium was also complicated by the hyperfine structure of the atomic levels involved in the absorption, complicating the curve fitting for the single-detector scheme used in this measurement. For our flux measurement, hyperfine splittings were measured in the experiment and used as constants for further curve fitting. The same Doppler linewidth was assumed for all hyperfine components.

Figure 11 is a measured relation between the ratio of the populations in the two levels and the QCM rate at different pressures. The result shows the tendency to more cooling when the rate was increased, consistent with the expansion cooling model, i.e., more population in the metastable level relaxes to the ground state level due to the cooling as the rate goes higher. The pressure dependence of the expansion cooling process is complicated by the fact that at higher background pressures, more e-beam power is needed to keep the rate constant, which increase the population in the metastable level, resulting in a process determined by interplay between the e-beam power and the collisional cooling, strongly depending on the source conditions.

Figure 12 shows that the combined flux, which was the summation of the flux independently measured at the two individual levels of yttrium, has a linear relation with the QCM rates at different background pressures of the argon gas. From this result, we conclude that by using two lasers the present scheme can provide a pressure-independent flux measurement.

The combined flux for yttrium in this article is a weighted summation of the atomic flux measured at two levels. To obtain the precise total flux, this weighting factor should be calibrated with either a precise ratio of the absorption cross sections of the two transitions or a vapor source with a known population ratio of those two levels, which could be determined by the temperature in a well-thermalized vapor.

At higher pressure, a larger scatter in the combined flux was observed (Fig. 12) that was attributed to the spatial variations of the atomic plume along the direction of the laser beams which cause the decorrelation between the QCM value and the line-integrated value obtained from the laser AA. The spatial variations may be caused by changes of the source condition and the scattering. The latter causes additional changes in the absorption path length. The scattering-induced effect was confirmed by comparing the measurements with different baffle widths for a given gap between the laser beams and the baffle, indicating that the measurement can be improved by minimizing the space between the baffle and the laser beams. Figure 13 shows another evidence of the significance of the scattering effect due to the background gas in the yttrium evaporation experiment at different pressures by putting the argon gas into the chamber. Two QCMs were separated by 13 cm and one of them was not directly exposed to the atomic plume (see the inset of Fig. 13). The measurement was performed at a deposition rate about 10 Å/s. All the pressures in this article were measured by a pressure gauge in the chamber far from the QCM. This result also indicates that the local pressure at the monitors is likely higher than that measured on a gauge far from the QCM.

D. Discussion on practical issues in AA sensor applications

1. Calibration

Calibration is necessary and nontrivial for the AA sensor to convert the measured quantity to the true deposition rate

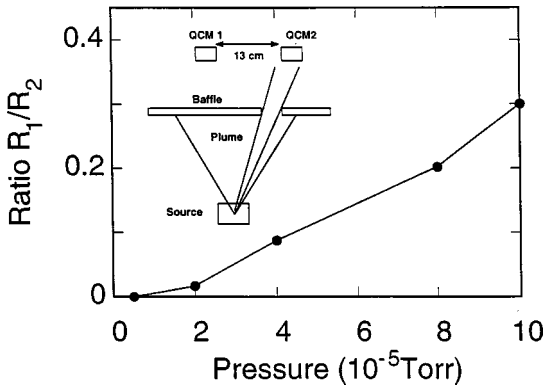

FIG. 13. R_1/R_2 vs the background pressure for yttrium evaporation. R_1/R_2 is the ratio of the measured deposition rates in QCM1 and QCM2, respectively. The distance between the two QCMs was about 13 cm. Note that QCM1 was not exposed to the atomic plume based on the geometry.

for a particular element. A QCM is usually used for this purpose. Careful comparison between the flux measured by the AA sensor and by the QCM with an atomic beam filtered by a small aperture inside the chamber shows an agreement within 1% accuracy.[13] It should be realized that the accuracy of the flux measurement with AA monitors applied to a large atomic plume cannot be completely evaluated by comparison with the flux measured by a single QCM, because the QCM and the AA sensor are not measuring exactly the same quantity. The QCM measures a local flux while the AA sensor measures the average flux over the entire absorption path length. Discrepancy between the AA sensor and QCM has been sometimes observed, and generally appears attributable to the spatial variation of the atomic flux in the e-beam evaporation process causing decorrelation between the QCM and the AA measurements.

As we have shown that the oxidation of the deposited material on QCM is observed in the experiment with oxygen background, the calibration for the AA sensor has to be performed at high vacuum condition.

The atomic density instead of the true flux measurement has been employed in many applications but can be problematic. The underlying assumption is that the normal velocity component remains constant with changes in the deposition conditions. This is not always true and not easy to calibrate out, depending on the accuracy required in the application. Understanding of the deposition process is crucial in selection between the more precise flux or the simpler density measurement approach. As we have shown for e-beam evaporation, the increase in velocity with increasing deposition rate is affected by the collision process of the atoms, so it is a function of the rate and the background gas pressure. In addition, for some high rate multielement deposition applications, the plume-plume interaction also makes the measurement of the appropriate velocity component indispensable.

In the use of AA sensors, one parameter should be clarified, i.e., the absorption path length which is the length of the laser beam intercepted by the atomic plume. In practical situations, one or more baffles are usually installed between the evaporation source and the substrate, which defines the effective path length. However, as we have shown experimentally, in the case that the deposition is performed in high background pressures, any change of the local pressure leads to a path length change due to the scattering effect, which is relatively hard to calibrate. Practically, shields have to be designed based on the evaporation conditions to suppress such variations.

In addition, in reactive deposition processes, there is a concern that the chemical reactions happen in the gas phase causing deviation of the AA measurement because the AA sensor only measures neutral atoms. Experimentally, there is no evidence to show reaction in gas phase in the cases investigated here when the background pressure of O_2 is up to 10^{-4} Torr.

As shown in the experimental results, some complications in the use of AA with some species may come from the existence of low-lying metastable levels close to the ground state. Simplification of flux measurement for the elements with metastable levels is desired. Modeling out the cooling process to eliminate the need for the second laser to monitor the metastable level, however, requires detailed understanding of the cooling process, and may not be practical in general.

The observations of the complexity of the source dependent evaporation process suggested that further systematic investigation of the spatial variation of the atomic plume and the source-dependent virtual source by tomographic or fluorescence imaging of the atomic plume are necessary.

2. Robustness of the AA sensors

The robustness of the AA sensor is characterized by the reproducibility of the measurement. AA measurements performed by using a hollow cathode lamp as an atomic source shows that the reproducibility was within 1%. The resolution of the AA sensor, which is determined by the available signal-to-noise ratio, is better than 1% at an absorption $<1\%$, corresponding to a deposition rate of 1 Å/s with an absorption path length of 1 cm in Ba and Y. In ECDL based AA spectroscopy with balanced detection, intensity and frequency noise are suppressed to close to the shot noise limit. Unlike the lamp-based AA system, optical alignment and coupling between optical components including the optical fibers in laser-based AA sensors are greatly relieved due to the relatively high power and the high spatial coherence of the laser beams. The real limit of sensor sensitivity is generally stray etalons in the system resulting from all surfaces of the optical components including chamber windows, which leads to a frequency-dependent variation in the baseline. Another noise source is the vibration of the vacuum system in the detection bandwidth which is coupled into optical signal through optical or microphonic effects. Use of the detection band at higher frequency region is an effective method to deal with low frequency noise,[14] but usually also leads to a more complicated system. The long term stability of the sensor relies on the performance of the PZT device used for modulating the laser frequency, and other electronic compo-

nents like the detectors and the amplifiers. The former is more susceptible and can be monitored and calibrated by an external etalon as a frequency reference. For the present application, the long-term drift of the absolute laser frequency does not have any consequence as long as the entire absorption spectrum can be scanned.

3. Availability of diode lasers for the AA sensors

Although the cost of diode lasers is becoming a lesser issue, another problem preventing wide extension of the laser based AA sensors is the unavailability of lasers for technologically interesting elements. At present, combinations of diode lasers and the diode-laser-based nonlinear frequency conversion can provide coherent radiation from the infrared to the UV, and are becoming a routine technology. We have previously demonstrated such type of AA sensor for the physical vapor deposition process in aluminum at 394 nm by using a frequency-doubled laser,[15] showing the promising technique with wider spectral coverage to provide availability for many important elements such as In (410 nm), Ga (403 nm), Cu (325 nm), Ti (381 nm),[7] etc.

IV. CONCLUSIONS

We have developed diode-laser-based AA spectroscopy monitors for true flux instead of simple density measurement, which is important for PVD process control. Laser beam schemes are designed for direct measurement of the velocity component normal to the substrate based on the Doppler shift measurement. *In situ* AA spectroscopy of two elements, barium and yttrium which are components in YBCO superconductor, has been performed to measure directly the atomic flux in e-beam evaporation. Experimental results show that a model-independent flux measurement was achieved by using a cross-beam scheme, while a counter-propagating-beam scheme with simpler instrumental configuration and interface with the chamber provides a flux measurement for a symmetric atomic plume. Both schemes have demonstrated pressure independence by using the flux rather than the simple density. In addition, the AA sensor was also used for diagnosing and helping better understand the deposition physics such as sticking coefficient, velocity of the evaporated atoms, and the oxidation of the elements on the substrate, enabling this technique for wider range of applications in both industrial PVD rate control and study of dynamics of deposition processes.

ACKNOWLEDGMENTS

This work has been supported by DARPA through Focus Research, Inc., Conductus, Inc., 3M Corp., National Science Foundation, the Center for Nonlinear Optics and Material, and the Center for Material Research at Stanford University. The authors also thank V. Matijasevic and J. Storer for various help and discussions.

[1]C. Lu, J. Vac. Sci. Technol. **12**, 578 (1975).
[2]J. E. Pollard and R. B. Cohen, Rev. Sci. Instrum. **58**, 32 (1987).
[3]H. Schwarz, Rev. Sci. Instrum. **32**, 194 (1961); R. H. Hammond, IEEE Trans. Magn. **MAG-11**, 201 (1975).
[4]C. Lu, M. J. Lightner, and C. A. Gogal, J. Vac. Sci. Technol. **14**, 103 (1977).
[5]S. J. Benerofe, C. H. Ahn, M. M. Wang, K. E. Kihlstrom, K. B. Do, S. B. Arnason, M. M. Fejer, T. H. Geballe, M. R. Beasley, and R. H. Hammond, J. Vac. Sci. Technol. B **12**, 1217 (1994).
[6]C. Lu and Y. Guan, J. Vac. Sci. Technol. A **13**, 1797 (1995); M. E. Klausmeier-Brown, J. N. Eckstein, I. Bozovic, and G. F. Virshup, Appl. Phys. Lett. **60**, 657 (1991).
[7]L. V. Berzins, Proc. SPIE **2068**, 28 (1994); L. V. Berzins, T. M. Anklam, F. Chambers, S. Galanti, C. A. Haynam, and E. F. Worden, Surf. Coat. Technol. **76-77**, 657 (1995).
[8]A. C. G. Mitchell and M. W. Zemansky, *Resonance Radiation and Excited Atoms* (Cambridge University Press, Cambridge, 1962), pp. 95–96.
[9]W. Wang, R. H. Hammond, M. M. Fejer, S. Arnacon, M. R. Beasley, M. L. Bortz, and T. Day, Appl. Phys. Lett. **71**, 31 (1997).
[10]A QCM measures the mass flux over a certain period of time. By assuming the density of the deposited film is equal to the corresponding bulk material, the deposition rate can be calculated, that has been performing in a conventional QCM instrument. Because the deposition rate Å/s is widely used in PVD process control, we used the deposition rate which is proportional to the atomic flux for a given species, to compare with our AA-based flux measurements.
[11]N. Uetake, T. Asano, and K. Siziki, Rev. Sci. Instrum. **62**, 1942 (1991).
[12]A. Nishimura, H. Ohba, and T. Shibata, J. Nucl. Sci. Technol. **29**, 1054 (1992).
[13]Per J. Slycke, Master degree thesis, 1998, University of Twente, The Netherlands; Conductus Inc. Internal Report of DARPA HTMA Project, 1998.
[14]W. Wang, R. H. Hammond, M. M. Fejer, C. H. Ahn, M. R. Beasley, M. D. Levenson, and M. L. Bortz, Appl. Phys. Lett. **67**, 1375 (1995).
[15]W. Wang, M. M. Fejer, R. H. Hammond, M. R. Beasley, and C. H. Ahn, M. L. Bortz, and T. Day, Appl. Phys. Lett. **68**, 729 (1996).